Integration of direct carbon and hydrogen fuel cells for highly efficient power generation from hydrocarbon fuels

Nazim Muradov*, Pyoungho Choi, Franklyn Smith, Gary Bokerman

Florida Solar Energy Center, University of Central Florida, 1679 Clearlake Road, Cocoa, FL 32922-5703, USA

ARTICLE INFO

ABSTRACT

In view of impending depletion of hydrocarbon fuel resources and their negative environmental impact, it is imperative to significantly increase the energy conversion efficiency of hydrocarbon-based power generation systems. The combination of a hydrocarbon decomposition reactor with a direct carbon and hydrogen fuel cells (FC) as a means for a significant increase in chemical-to-electrical energy conversion efficiency is discussed in this paper. The data on development and operation of a thermocatalytic hydrocarbon decomposition reactor and its coupling with a proton exchange membrane FC are presented. The analysis of the integrated power generating system including a hydrocarbon decomposition reactor, direct carbon and hydrogen FC using natural gas and propane as fuels is conducted. It was estimated that overall chemical-to-electrical energy conversion efficiency of the integrated system varied in the range of 49.4–82.5%, depending on the type of fuel and FC used, and CO_2 emission per kW_{el} h produced is less than half of that from conventional power generation sources.

1. Introduction

Hydrocarbon-based fuels will remain one of the major sources of electrical power generation in the near-to-mid term future. In view of ever increasing cost of hydrocarbon fuels coupled with a negative environmental impact of their combustion products, it is imperative to significantly increase the energy conversion efficiency of hydrocarbon-based power generation systems. Fuel cells (FC) are considered to be the most efficient energy conversion devices, compared to conventional power generators based on internal combustion and diesel engines, turbines, etc. Due to a number of intrinsic chemical characteristics and non-polluting nature, hydrogen is the most commonly used fuel in commercial FC, such as alkaline, phosphoric acid and proton exchange membrane (PEM) FC. High-temperature FC, e.g., molten carbonate and solid oxide FC (SOFC) can use a variety of fuels including hydrogen, carbon monoxide and light hydrocarbons.

Recently, a wide range of hydrocarbon reformers (HR) of different designs and capacities have been developed for stationary, distributed and mobile (on-board) FC applications (e.g., Refs. [1–3]). The vast majority of HR are based on three hydrocarbon processing technologies: steam reforming, partial oxidation and autothermal reforming. HR are complex multi-unit devices involving production of syngas followed by its conditioning/purification to hydrogen (or hydrogen-rich gas). Depending on the hydrocarbon feedstock and operational parameters, the chemical-to-hydrogen energy conversion efficiencies of commercial reformers vary in the range of 60–80% [4]. Assuming HR efficiency of 80%, and hydrogen-to-electricity (optimistic) conversion efficiencies of 50 and 60% for low- and high-temperature FC [4], respectively, the combined HR-FC systems would yield the overall energy conversion efficiency of $0.8 \times 0.5 \times 100\% = 40\%$ for PEMFC, and $0.8 \times 0.6 \times 100\% = 48\%$ for SOFC. Thus, the overall energy conversion efficiency of the existing (conventional) HR-FC-based power generation systems is unlikely to exceed 45–50% (without co-generation). Evidently, these values do not represent a dramatic increase in the efficiency over that of advanced power generators utilizing diesel engines or gas turbines (35–40%). Thus, significant improvement in the energy conversion efficiencies of hydrocarbon-based power generation systems is necessary.

Although the most of FC-related activities are still focused on hydrogen-fueled FC (H$_2$FC), direct carbon FC (DCFC) are increasingly attracting attention of researchers due to potentially much higher fuel energy conversion efficiency compared to H$_2$FC. It is important to note that as fuel carbon has the highest volumetric energy density ($19 \, kWh \, L^{-1}$) among all electrochemically active fuels, battery anodes and transportation fuels (compared to: H$_2$: $2.4 \, kWh \, L^{-1}$; Zn: $9.3 \, kWh \, L^{-1}$; Li: $6.9 \, kWh \, L^{-1}$; gasoline: $9.0 \, kWh \, L^{-1}$; diesel: $9.8 \, kWh \, L^{-1}$ [5]). In DCFC, solid carbon is introduced to the anode compartment where it is electro-oxidized to CO_2 generating electricity:

$$C + O_2 \rightarrow CO_2 \qquad E^o = 1.02 \, V \qquad (1)$$

* Corresponding author. Tel.: +1 321 638 1448; fax: +1 321 638 1010.
E-mail address: Muradov@fsec.ucf.edu (N. Muradov).

Nomenclature

CTE   chemical-to-electrical
C_B H_2 bulk concentration in the H_2–CH_4 mixture
$(CO_2)_{TCD}$ CO_2 emission from TCD process
DCFC   direct carbon fuel cell
D diffusion coefficient of H_2
d_{002} interlayer distance in carbon
FC   fuel cell
GT   gas turbine
E_{in} energy input
HR   hydrocarbon reformer
H_2FC hydrogen-fueled fuel cell
HHV   higher heating value
$\langle H_2 \rangle$ hydrogen yield per unit of methane
i current flowing through the cell
i_L limiting current
LPG   liquefied petroleum gas
OCP   open circuit potential
NG   natural gas
n the number of electrons transferred in the cell reaction
PGC   plasma-generated carbon
PEMFC   proton exchange membrane fuel cell
R universal gas constant
SOFC   solid oxide fuel cell
ST   steam turbine
TCD   thermocatalytic decomposition
V, V_o operating and open circuit voltages of a fuel cell, respectively.
W_{el} electrical energy input to the process

Greek symbols
ΔH_{TCD} enthalpy of methane decomposition reaction at operational temperature
ΔH_{H_2}, ΔH_{carbon}, ΔH_{CH_4} higher heating values of H_2, carbon and methane, respectively
ΔG, ΔH, ΔS free energy, enthalpy and entropy of carbon oxidation reaction
$\Im$ Faraday constant
δ thickness of the diffusion layer
ϕ thermal efficiency of the TCD reactor
φ thermal-to-electrical energy conversion efficiency
η_{FC} actual efficiency of a fuel cell
η_{eff} overall energy efficiency
η_{conc} concentration polarization
ξ electrical efficiency of the plasma device
μ_{fuel} fuel utilization coefficient
μ molecular weight
ψ CO_2 emissions resulting from generation of electric power

The actual efficiency of DCFC could be defined as follows:

$$\eta_{FC} = \frac{\Delta G(T)}{\Delta H}\mu_{fuel}\frac{V}{V_o} = \frac{\Delta G(T)}{\Delta G + T \, \Delta S}\mu_{fuel}\frac{V}{V_o} \qquad (2)$$

where η_{FC} is FC actual efficiency, ΔG, ΔH and ΔS are free energy, enthalpy and entropy of the reaction (1), μ_{fuel} is a fuel utilization coefficient, V and V_o are operating and open circuit voltages of FC, respectively.

Since $\Delta S \approx 0$ for the reaction (1), and assuming that for DCFC $\mu_{fuel} \approx 1.0$ and $V/V_o \approx 0.8$, the overall fuel energy conversion efficiency of DCFC in practical systems is estimated at 80% [6]. It should be noted that energy conversion efficiency of about 80% has already

been demonstrated on the laboratory scale DCFC using different types of carbon [7], and the efficiency could potentially reach up to 90% upon further development of the technology. Recently, different types of DCFC utilizing a variety of electrolytes in a different temperature range have been under the development. In particular, SOFC with yttria stabilized zirconia as an electrolyte operating at temperatures of 900–1000 °C [8], molten salt electrolyte FC operating at 600–800 °C [9], and combined SOFC and molten carbonate FC operating in the temperature range of 525–700 °C [10], have been reported. Thus, DCFC enjoy the following advantages over other types of FC: (i) the highest theoretical (~100%) and practical fuel energy conversion efficiencies, (ii) the highest fuel utilization efficiency (since the fuel—carbon and the product CO_2 exist in separate phases, allowing full conversion of carbon in a single pass), and (iii) CO_2 is produced in a concentrated form ready for liquefaction, transportation and sequestration.

Despite the advantages of DCFC over H_2FC in terms of significantly higher fuel energy conversion efficiency, the widespread practical implementation of DCFC is hindered by several factors mostly related to the system sustainability, and the need for the supply of clean (i.e., sulfur- and ash-free) carbon fuel. From this viewpoint, the use of hydrocarbon fuels as a source of pure carbon for DCFC would be advantageous, however, up to date, no technology is available for sustainable production of both hydrogen and clean carbon from hydrocarbons at the practical range of temperatures (below 1000 °C). The objective of this work is to develop a highly efficient integrated energy conversion system based on decomposition of hydrocarbon fuels to hydrogen and clean carbon that are separately utilized, respectively, in hydrogen- and carbon-powered fuel cells.

2. Description of the concept

The proposed concept is based on the combined operation of a thermocatalytic hydrocarbon decomposition (TCD) reactor with hydrogen- and carbon-fueled FC. In the TCD reactor, a hydrocarbon feedstock (e.g., methane) is catalytically decomposed to H_2 (or hydrogen-rich gas) and carbon at the temperature range of 800–900 °C. H_2 or hydrogen-rich gas is used as fuel in H_2FC, whereas, the clean carbon product is withdrawn from the TCD reactor and used in DCFC, as shown below:

$$CH_4 \xrightarrow{\text{catalyst}} 2H_2 + C \quad \begin{matrix} \nearrow H_2FC \\ \searrow DCFC \end{matrix} \qquad (3)$$
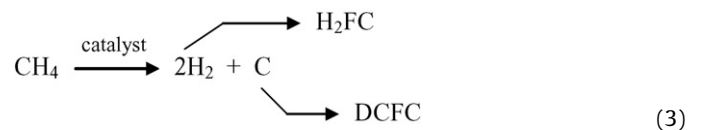
Due to the absence of oxidants (steam, oxygen) in the reactor no carbon oxides (CO_x) are formed, thus, eliminating a need for water gas shift and CO_2 removal units. In principle, the concept is applicable to any gaseous or liquid fuel, e.g., natural gas (NG), liquefied petroleum gas (LPG), gasoline, diesel fuel, etc. The concentration of hydrogen in the gaseous product depends on the nature of the hydrocarbon feed and operating conditions (temperature, pressure, residence time) in the TCD reactor: higher temperature and residence time typically result in higher H_2 concentration in the effluent gas (which could vary in the range of 30–80 vol.%, the balance being predominantly methane with small amounts of C_2 hydrocarbons).

Thermocatalytic decomposition of hydrocarbons over metal- and carbon-based catalysts is an active area of research. Of particular interest is decomposition of NG (consisting mostly of methane), however, the practical realization of the process faces several technical challenges. In particular, the main two problems with the use of metal-based catalysts relate to their rapid deactivation due to carbon deposition on active sites and difficulty of separating
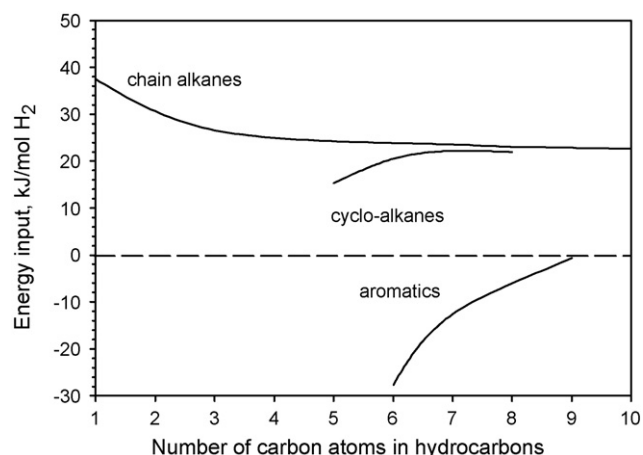
Fig. 1. Energy input required to extract one mole of H_2 (at standard conditions) from different classes of hydrocarbons as a function of number of carbon atoms in hydrocarbons.

carbon from metal catalyst particles (in most cases, the metal nanoparticles are incorporated into carbon microstructure). Although carbon catalysts offer certain advantages over metal catalysts due to their high durability (sulfur and temperature resistance) and low cost, they are also prone to deactivation which is attributed to the build up of a catalytically inactive turbostratic form of carbon [11].

Catalytic decomposition of C_2+ hydrocarbons and commercial hydrocarbon fuels (e.g., NG, LPG, gasoline, diesel) is much less researched area. Commercial liquid fuels (gasoline, diesel) contain different classes of hydrocarbons (paraffins, cyclo-alkanes, alkyl-aromatics, etc.), that have dissimilar energy input requirements for extracting hydrogen from them. Fig. 1 shows the dependence of energy input (E_{in}) required to extract one mole of H_2 (at standard conditions) from different classes of hydrocarbons as a function of a number of carbon atoms in hydrocarbon. It can be seen that the energy input requirement per mole of H_2 extracted from aliphatic hydrocarbons (or alkanes) is decreased with the increase in their molecular weight; the most significant drop in the E_{in} value occurs during transition from methane to propane, and for alkanes higher than butane, the E_{in} value almost levels up. E_{in} values for cyclo-alkanes show a reverse trend, which can be explained by lesser energetic stability of lower (i.e., C_4 and C_5) cyclo-alkanes compared to C_6. Interestingly, the decomposition of aromatic and some of alkyl-aromatic hydrocarbons is an exothermic process (i.e., no energy input is required); the increase in the molecular weight of alkyl moiety in alkyl-aromatic hydrocarbons results in the increase in the E_{in} value with the overall process approaching thermo-neutrality. One important conclusion that can be drawn from the analysis of this diagram is that, in general, amount of energy required to extract H_2 from hydrocarbons via decomposition reactions is relatively low compared to other reforming technologies (e.g., for methane and propane decomposition it corresponds to 8.5 and 5.5% of their respective higher heating values, compared to 28% for the steam methane reformation process).

3. Experimental

Reagents. Methane (99.999% purity), hydrogen (certified grade of 99.999%) and argon (99.999%) were received from Air Products and Chemicals, Inc. Pipeline-quality NG (also called, industrial methane) was obtained from Holox Inc. and used without a further treatment or purification. The composition of the NG feedstock used in the experiments was as follows: (vol.%) methane 93.1, ethane 4.1, propane 0.7, C_4+ 0.3, N_2 0.9, CO_2 0.9, H_2S 4 ppm. Propane

(99.9% purity) was obtained from Praxair. The sample of carbon black Black Pearl 2000 (surface area 1500 m^2 g^{-1}) was obtained from CABOT Corp. and used "as received". Commercial diesel fuel was purchased from a local gas-filling station. The samples of activated carbons (AC) were obtained from Fisher and NORIT Americas. A stainless steel (70Fe–19Cr–11Ni) wire (1.0 mm in diameter) was obtained from Alfa Aesar and used as an electrode material in a non-thermal plasma reactor. Ru (0.5 wt.%)/Al_2O_3 was obtained from Aldrich Chemical Co. and used in CO methanation experiments. NiO (1–15 wt.%)/Al_2O_3 was obtained from Süd-Chemie Inc. and used in ethylene hydrogenation experiments (the catalyst was hydrogenated in a stream of H_2 before its use in the ethylene hydrogenation reaction). The above catalysts were used in the form of 10–18 mesh granules. ZnO pellets obtained from Süd-Chemie Inc. were used for removing H_2S from NG decomposition gas.

Experimental procedure. The experiments on carbon-catalyzed decomposition of hydrocarbon feedstocks were conducted using fixed and moving bed reactors. In the fixed bed reactor arrangement, carbon catalysts were placed on a ceramic support inside the TCD reactor, and hydrocarbon (e.g., methane, NG, propane and diesel fuel) was decomposed over the catalyst layer producing gaseous products exiting the reactor and carbon remaining inside the reactor. The fixed bed reactors were made of quartz (OD = 12 mm) or high-temperature alloy (OD = 2.5–5.0 cm). The amount of carbon catalyst in the TCD reactor was: 0.1–10.0 g, depending on the size of the reactor. The reactors were maintained at constant temperature via a type K thermocouple and Love Controls microprocessor. All experiments were conducted at atmospheric pressure. Before the experiments, all carbon samples were heated at 500 °C for 0.5 h and 850 °C for another 0.5 h in a stream of Ar to remove all the adsorbed and pore-entrained oxygen and water from the carbon surface. Hydrocarbon decomposition experiments were conducted in the temperature range of 800–900 °C, and the residence time range of 1–20 s (in the carbon bed).

The experimental unit for conducting NG decomposition over the fixed bed of carbon catalyst consists of a thermocatalytic reactor (OD = 5 cm) made of Inconel alloy, a bag filter, an H_2S scrubber, C_2H_4 hydrogenation reactor and a methanator. Gas desulfurization was conducted using ZnO granules placed in a stainless steel reactor (OD = 2.5 cm) and heated to 350 °C. Ethylene hydrogenation (over Ni/alumina catalyst) and CO methanation (over Ru/alumina catalyst) were conducted in stainless steel reactors (OD = 2.5 cm) heated to 150–200 and 350 °C, respectively. In the moving bed (or vortex-flow) reactor arrangement, a hydrocarbon feedstock (e.g., NG) was introduced into the reactor along with the flow carbon aerosols produced by a non-thermal plasma device attached to the TCD reactor. Plasma-generated carbons (PGC) were produced by a modification of Gliding-Arc technique (described in Ref. [12]) using an in-house fabricated non-thermal plasma device including a high-voltage power source and two stainless steel electrodes [13]. The plasma device was attached to the hydrocarbon decomposition reactor such that the carbon aerosols and the gaseous products of plasma-assisted decomposition of hydrocarbon were directed to a vortex-flow reactor, where at elevated temperatures (850–900 °C) carbon-catalyzed decomposition of hydrocarbon took place. The vortex-flow reactor (OD = 5 cm) was made of a high-temperature alloy Inconel.

PEM fuel cell performance measurements. A four-cell PEMFC stack was assembled from parts provided by Fuel Cell Technologies Inc. and tested using different H_2–CH_4 mixtures. An individual cell consists of a 25 cm^2 single serpentine flow field on both anode and cathode. In measuring polarization curves, current was stepped up from zero to the maximum test current density with an increment between 10 and 100 mA cm^{-2}. Time spent at each current density was 5 min. A 100A Model 890B Scribner load box (Scribner Associates, Southern Pines, NC) with a built-in current interrupt
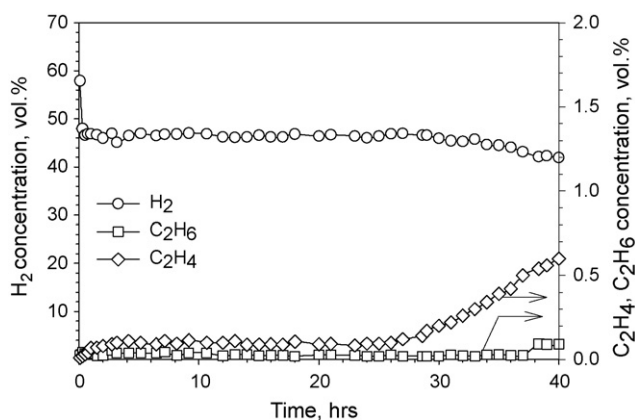
Fig. 2. Thermocatalytic decomposition of methane over plasma-generated carbon. $T = 890\,°C$.

Fig. 3. Thermocatalytic decomposition of propane over plasma-generated carbon. $T = 860\,°C$.

resistance measurement was used for the polarization measurements. The anode and the cathode gas line temperatures were set 10 °C above the cell temperature to prevent water condensation in the inlet gas lines. The product water in the cells was recycled to internally humidify the stack. Thin polymer membranes were used as a separator between the humidified exit gases and dry inlet gas. Such a humidification scheme does not appreciably add to the parasitic loss from the overall system.

Products analysis and characterization. Analysis of the gaseous products generated in the hydrocarbon decomposition reactor was performed using gas chromatographs: SRI-8610A GC (thermal conductivity detector, argon carrier gas, silica gel packed column) and a Varian-3400 GC (flame ionisation detector, helium carrier gas, HysepD$_B$ packed column). The microstructure of carbon samples was examined by transmission electron microscopy (TEM) (Tecnai F30, 300 kV field emission source, equipped with STEM, HAADF detector and XEDS, manufacturer: FEI/Philips). X-ray diffraction (XRD) analysis of the PGC samples was conducted using Rigaku D-MaxB diffractometer. Analysis of sulfurous compounds was conducted using Perkin Elmer GC (flame photometric detector, capillary column). Additionally, H$_2$S content in the hydrocarbon decomposition gases was determined with the use of Sensidyne® gas detection tubes (the detection range: 0.2–5 ppm H$_2$S).

4. Results and discussion

4.1. Carbon-catalyzed decomposition of hydrocarbons

From the viewpoint of carbon utilization in DCFC, the use of carbon-based catalysts in the TCD process is more advantageous compared to metal catalysts because it allows producing a clean carbon product not contaminated by metal particles or other inorganic impurities. Thus, in this work, the main focus was on the development of carbon-catalyzed thermocatalytic hydrocarbon decomposition process. Fig. 2 shows the results of methane decomposition (890 °C) over carbon particles produced by non-thermal plasma-assisted decomposition of methane in a fixed bed reactor (for simplicity, unconverted methane is not shown on the graph). It can be seen that initially hydrogen concentration rapidly (in less than one hour) dropped to a quasi-steady state level of about 46 vol.%, at which it remained for about 26 h followed by a gradual decline. C$_2$H$_6$, C$_2$H$_4$ concentrations stayed at the low level of less than 0.1 vol.% over about 25 h, followed by a gradual increase in C$_2$H$_4$ concentration (C$_2$H$_6$ concentration remained at the same low level). The carbon product yield was determined by subtracting the weight of original carbon catalyst from the total weight of carbon collected from the reactor after the methane decomposition exper-
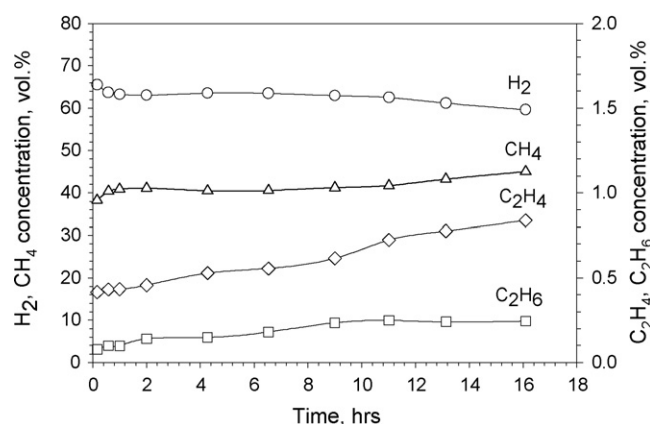
iment. The carbon balance was closed within the margin of error of 6–8%.

Fig. 3 depicts the distribution of gaseous products of TCD of propane at 860 °C using PGC catalyst. Hydrogen concentration in the effluent gas is increased compared to methane decomposition reaching up to 66 vol.% at the onset and about 63 vol.% at the quasi-steady state of the reaction, and remained at that level for about 10 h before starting a slow decline in value. The yields of C$_2$ hydrocarbons produced from propane are also higher compared to methane decomposition with C$_2$H$_4$ concentration reaching up to about 1 vol.% at the end of the experiment. TCD of diesel fuel over the fixed bed of activated carbon (coconut) catalyst was carried out at 800 °C. The hydrogen concentration in the effluent gas at the onset of the process was 63.2 vol.% with balance being methane and small amounts (less than 0.5 vol.%) of C$_2$ hydrocarbons (some trace amounts of CO$_x$ were also present, most likely, originated from oxygenated additives and moisture impurities in diesel). However, as the process progressed, H$_2$ concentration slowly decreased and methane concentration increased along with the concentration of C$_2$ (especially, C$_2$H$_4$) hydrocarbons. The above experiments clearly point to unsustainable nature of the diesel TCD process over activated carbon catalyst in the fixed bed reactor arrangement.

Of particular practical interest is TCD of NG due to its availability (a pipeline delivery network) and relatively low cost (compared to other hydrocarbon feedstocks). Besides methane and other hydrocarbons (ethane, propane and butanes), NG typically contains certain amounts of nitrogen, CO$_2$ (from few tenths to several volume percents) and a few ppm of sulfurous compounds (H$_2$S, mercaptans). This imposes several limitations to the use of the hydrogen-rich gas from the NG-fed TCD process in PEMFC as follows. To avoid poisoning of PEMFC anode catalyst (Pt) sulfurous compounds (e.g., H$_2$S) have to be scrubbed down to ppb levels (according to the FreedomCAR hydrogen fuel specifications, H$_2$S concentration in it is limited to 10 ppb [14]) (note that in the reducing atmosphere of the TCD reactor at 850–900 °C, most of mercaptans are converted to H$_2$S). During high-temperature catalytic decomposition of NG, CO$_2$ impurities could react with hydrocarbons, or carbon catalyst forming CO, which even in very small quantities easily poisons the anode catalyst in PEMFC (a permissible CO concentration in an anode feed is below 10 ppmv [14]). Furthermore, C$_2$H$_4$ is also undesirable component in the anode feed gas as it may potentially deactivate the anode catalyst via the blockage of catalytic active sites and/or polymerization reactions (the ethylene concentration in the hydrogen feed is limited to 50 ppm). Thus, H$_2$–CH$_4$ mixture produced by NG catalytic decomposition has to be treated, first, by scrubbing H$_2$S by a ZnO bed, and, secondly, by hydrogenating ethylene to ethane and CO to CH$_4$ (via methanation
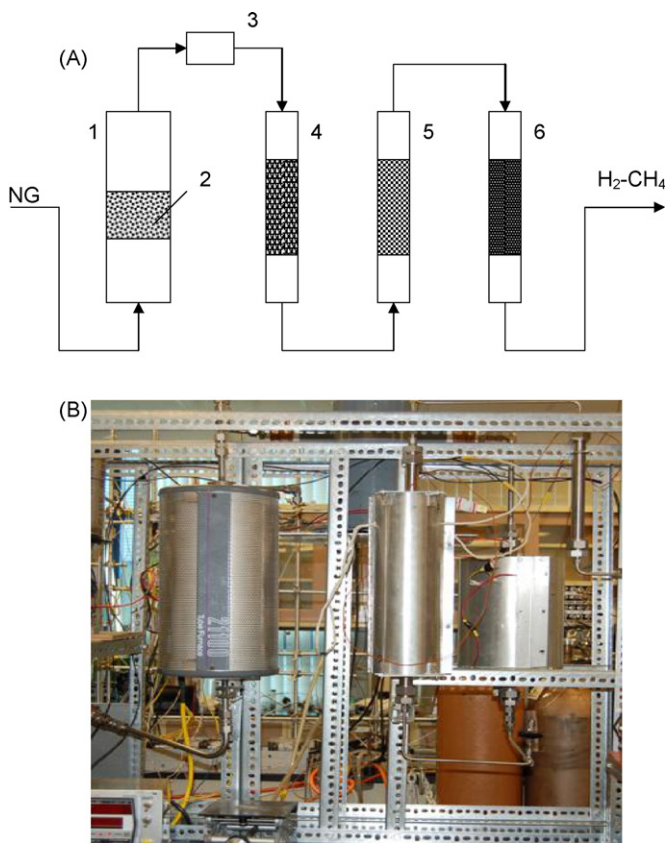
Fig. 4. Schematic (A) and photo (B) of the experimental unit for production of hydrogen-rich gas from pipeline natural gas. (1) A thermocatalytic reactor, (2) carbon catalyst, (3) a filter, (4) H$_2$S scrubber, (5) a hydrogenation reactor, and (6) a methanation reactor.
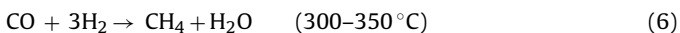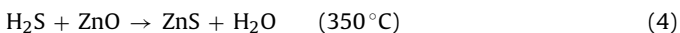
reaction) according to the following reactions:

$$H_2S + ZnO \rightarrow ZnS + H_2O \qquad (350\,^\circ C) \qquad (4)$$

$$C_2H_4 + H_2 \rightarrow C_2H_6 \qquad (150–250\,^\circ C) \qquad (5)$$

$$CO + 3H_2 \rightarrow CH_4 + H_2O \qquad (300–350\,^\circ C) \qquad (6)$$

Fig. 4 shows the schematic diagram (A) and the photograph (B) of the experimental unit for production of hydrogen-rich gas by TCD of NG in a fixed bed catalytic reactor (with the gas post-treatment). The unit consists of a thermocatalytic reactor (1), a bag filter to catch airborne carbon particles exiting the TCD reactor (3), an H$_2$S scrubber containing ZnO pellets (4), C$_2$H$_4$ hydrogenation reactor filled with Ni/alumina catalyst (5) and a methanator containing Ru/alumina catalyst (6). Although these gas purification/conditioning units add some complexity to the system, advantageously, they all operate in a "passive" regime (i.e., they do not require addition of any reagents), and are easy to control, which simplifies the process.

TCD of NG was conducted in the fixed bed reactor containing carbon-based catalysts: carbon black Black Pearl 2000 and activated carbon (Darco) at 860–880 °C and atmospheric pressure (Note that both Black Pearl 2000 and activated carbon catalysts contained small quantities of sulfurous and oxygenated compounds resulting in production of appreciable amounts of H$_2$S and CO during the initial stage of the process). Carbon produced during the process laid down on the surface of original carbon catalyst and remained in the reactor until the end of the experiment. The analysis of the effluent gases during NG decomposition indicated that CO concentration dropped from about 0.2–0.5 vol.% (after the TCD reactor) to 4–6 ppm (after the methanator). The concentrations of
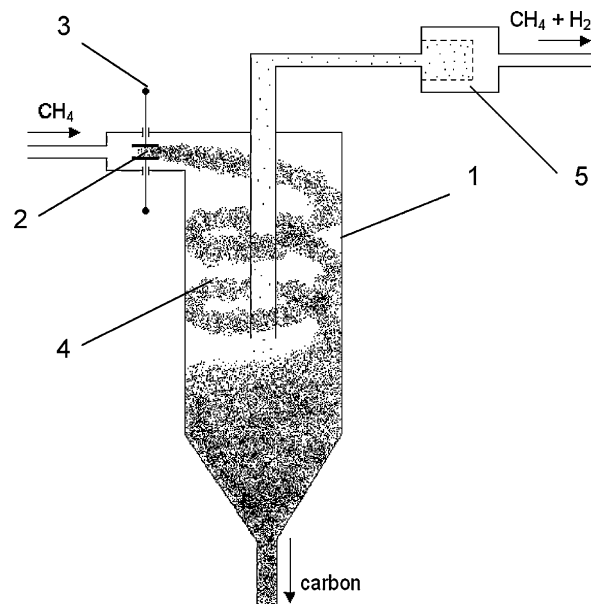

Fig. 5. Conceptual design of the vortex-flow TCD reactor with attached non-thermal plasma carbon generator. (1) A vortex-flow reactor, (2) plasma carbon generation area, (3) connectors to high-voltage power supply, (4) carbon aerosols and (5) a bag-type filter.

H$_2$S and ethylene in the hydrogen-rich gas at the end of the technological chain were below the detectable levels (less than 0.2 ppm) (The detection limits of the analytical methods used in this work did not allow detecting H$_2$S at the low ppb level, however, it is well known that ZnO can achieve almost complete removal of H$_2$S from sulfurous gases, and it is widely used in gas purification industry [15]). An average hydrogen concentration in the resulting H$_2$–CH$_4$ mixture was 40–55 vol.%, depending on the reaction temperature. After several hours of operation, however, H$_2$ concentration started slowly declining due to carbon catalyst deactivation. Propane produced H$_2$–CH$_4$ mixtures with somewhat higher H$_2$ concentration (about 55–65 vol.%), but the process also was not sustainable.

In order to improve the sustainability of the NG decomposition process, a vortex-flow TCD reactor with moving bed of carbon catalyst particles was utilized. To produce the continuous flow of the catalyst particles, a non-thermal plasma carbon-generating device was attached to the TCD reactor. In such an arrangement, the carbon aerosol particles produced by plasma-assisted NG decomposition are carried away by a gaseous stream and enter a vortex-flow TCD reactor via a tangential inlet port. In the vortex reactor, the swirling carbon aerosol particles catalyze NG decomposition at the temperature of 860–890 °C resulting in the production of H$_2$-rich gas (predominantly, H$_2$–CH$_4$ mixture) exiting the reactor via a coaxially located outlet tube connected to a bag-type filter. Carbon particles are accumulated in the lower section of the vortex reactor, from where they drop to a carbon collector. Fig. 5 shows a conceptual design of the vortex TCD reactor with the attached plasma carbon-generating device (the actual configuration of the apparatus may vary, depending on the specifics of the plasma device and vortex reactor). The NG decomposition experiments demonstrated that the process reached steady state condition in about 1 h and remained at that state for several hours. H$_2$ concentration in the effluent gas after the vortex TCD reactor varied in the range of 35–50 vol.%, depending on temperature and residence time in the vortex reactor (the balance being methane and small amounts, less than 1–2 vol.%, of C$_2$ hydrocarbons). Fig. 6 depicts the time dependence of hydrogen concentration in the effluent gas exiting from the TCD reactor (un-reacted methane and small amounts of C$_2$ hydrocarbons are not shown). Carbon particles formed in the TCD-
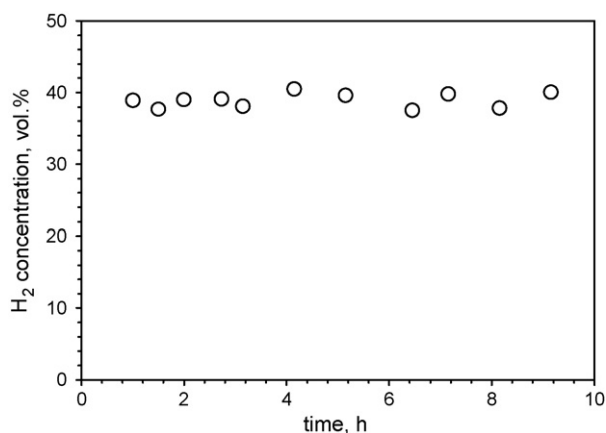
Fig. 6. Time dependence of hydrogen concentration produced by NG decomposition over plasma-generated carbons in the vortex-flow reactor. Temperature 870 °C.

Fig. 8. TEM image of carbon produced by thermocatalytic decomposition of methane over plasma-generated carbon catalyst.

vortex reactor were collected in a carbon collector and analyzed by a number of material characterization techniques.

It should be noted that a vortex-flow reactor (albeit, of a different design) was utilized for solar thermal decomposition of NG at elevated temperatures [16]. In some respect, the flow pattern in the vortex reactor is similar to that of industrial cyclones for separating fine solid particles from gaseous streams.

4.2. Characterization of carbon product and evaluation of its suitability to DCFC

The carbon product of the methane decomposition reaction was characterized and evaluated for its suitability to DCFC. XRD analysis of the carbon product revealed some three-dimensional structural ordering, as characterized by the intensive and relatively broad (0 0 2) XRD peak at the diffraction angle of about 25° 2θ and the interlayer spacing ($d_{0 0 2}$) of $d_{0 0 2}$ = 3.50–3.54 Å (Fig. 7). For comparison, X-ray diffractogram of perfectly ordered pure graphite (also included in Fig. 7) is characterized by a very sharp (0 0 2) diffraction peak at 26.3 degrees 2θ and d-spacing of $d_{0 0 2}$ = 3.348 Å. The TEM image of the TCD-produced carbon shows pronounced irregularities and the lack of particular structural order (Fig. 8). The above data point to semi-ordered structure of the TCD-generated carbon, which is typical of turbostratic carbon (i.e., in this type of carbon, the layers are roughly parallel and equidistant, but are not other-
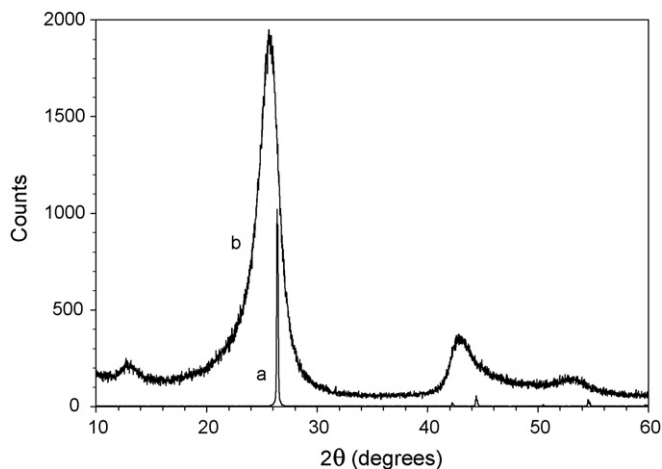
wise mutually oriented, and there are profound irregularities and defects within the graphene layers).

Although factors affecting the electrochemical activity of carbon materials in DCFC are still actively researched area, it was pointed out by many researchers that, in general, disordered carbons tend to be rather reactive in DCFC due to high concentration of defects and edge atoms (compared to those in the basal plane of carbon) (e.g., Ref. [9]). In particular, it was reported that turbostratic carbon exhibited unusually high electrochemical reactivity in molten carbonate-based DCFC [7]. Currently, the carbon samples produced by TCD of NG are being tested in DCFC; the results will be reported elsewhere.

4.3. Operation of TCD reactor coupled with PEM fuel cell

4.3.1. Operating PEMFC using H_2–CH_4 mixtures as anode feed

There is a lack of information in the literature on operating PEMFC using H_2–CH_4 mixtures as an anode feed. To determine the effect of methane on PEMFC performance, a four-cell FC stack was assembled and tested at 60 °C and atmospheric pressure using H_2–CH_4 mixtures with H_2 concentrations in the range of 40–100 vol.% as an anode feed (Fig. 9A and B). The results of testing are presented in Fig. 10A and B. In particular, Fig. 10A depicts open circuit potential (OCV) of the four-cell stack as a function of H_2 concentration in the H_2–CH_4 mixtures. It is clear from Fig. 10A that the OCV value slightly decreases from 3.63 to 3.44 V as the H_2 concentration decreases from 100 to 40 vol.% (for a single-cell system OCV values correspond to 0.91 and 0.86 V, respectively). The performance of the four-cell stack using H_2–CH_4 mixtures with H_2 concentration of 40, 60 and 100 vol.% is shown in Fig. 10B. The results of the FC testing indicate that there is no significant difference in the power output of the four-cell PEMFC stack operating on different H_2–CH_4 mixtures until the current densities of 200–300 mA cm^{-2} are reached. At higher current densities, the feeds containing lower concentration of hydrogen yield lower potential compared to the pure hydrogen feed. It is known that at practical current densities, slow transport of the reactant (H_2) to the electrochemical interface is a major contributor to concentration polarization, as evident from the following formula [17]:

$$\eta_{conc} = \frac{RT}{n\Im} \ln\left(1 - \frac{i}{i_L}\right) \qquad (7)$$

where η_{conc} is concentration polarization, R is universal gas constant, $\Im$ is Faraday constant, n is the number of electrons transferred in the cell reaction, i is the current flowing through the cell, i_L is the limiting current.

Fig. 7. XRD of carbon produced by thermocatalytic decomposition of methane over plasma-generated carbon catalyst. (a) graphite and (b) TCD carbon.
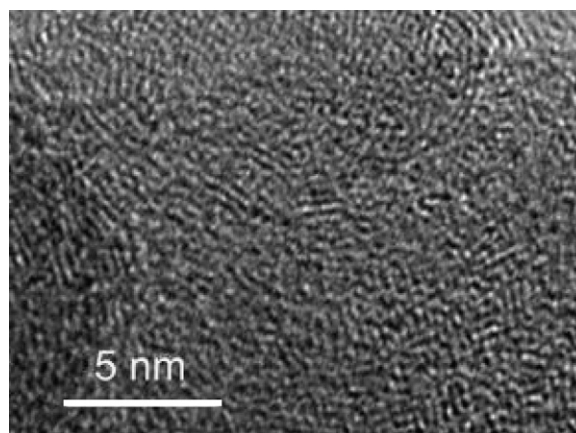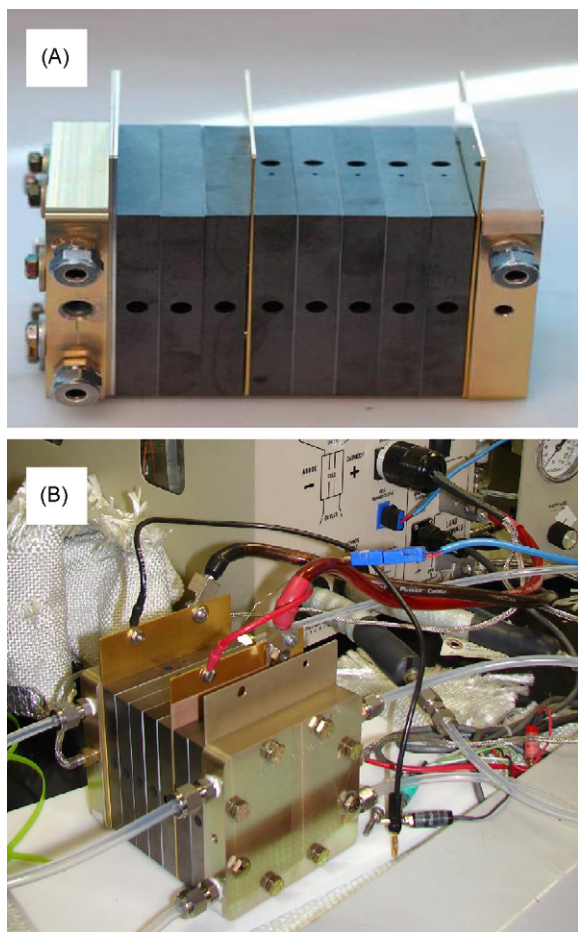
Fig. 9. (A) Four-cell PEMFC stack with an internal humidifier and (B) performance testing of the four-cell PEMFC stack using H_2–CH_4 mixtures.

Fig. 10. Four-cell PEMFC stack performance testing using H_2–CH_4 mixtures with different H_2 concentrations. (A) Open circuit voltage vs H_2 concentration and (B) FC current–voltage performance curves using different H_2–CH_4 mixtures.

The limiting current (i_L) is a measure of the maximum rate at which H_2 can be supplied to an electrode, and it is defined as follows:

$$i_L = \frac{n \Im D C_B}{\delta} \qquad (8)$$

where D is the diffusion coefficient of the reacting specie (H_2), C_B is H_2 bulk concentration in the H_2–CH_4 mixture, δ is the thickness of the diffusion layer.

It can be seen from formulae (7) and (8) that lower C_B values would result in lower values of the limiting current (i_L), and, hence, higher values of the concentration polarization (η_{conc}), thereby causing the cell voltage to drop. Thus, the operating range of the stack using H_2–CH_4 feed stream should be in a high potential region in which the fuel cell efficiency is relatively high.

The above results of the four-cell stack testing indicate that the presence of methane in the H_2–CH_4 feed does not adversely affect the performance of PEMFC beyond a mere dilution effect. Methane dilutes the hydrogen feed as any non-reactive gas causing change in Nernst voltage through the reduction of mole fraction of the active species, but it does not markedly interfere with the kinetics of hydrogen oxidation reaction.

4.3.2. Operating TCD reactor combined with PEMFC

In the next series of experiments, a single-cell PEMFC was fed by the H_2–CH_4 mixture generated by the TCD reactor with the fixed bed of PGC catalyst operating on pure methane as a feedstock (The use of a single cell instead of a four-cell stack was due to relatively low flow rate of the feed gas from the TCD reactor).
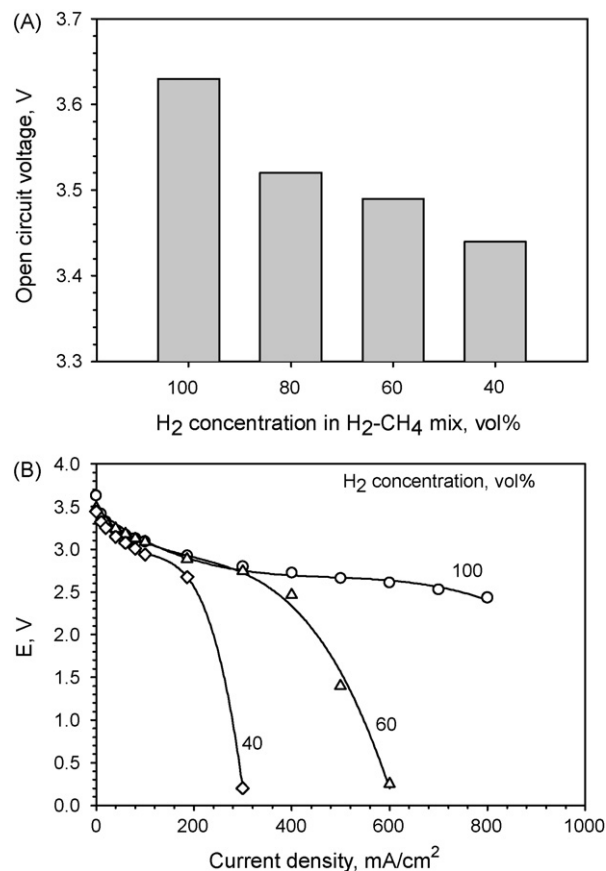
Temperature and residence time in the TCD reactor varied such that two H_2–CH_4 mixtures were produced: with H_2 concentration of 35 and 46 vol.% (the latter H_2-containing gas corresponds to the experiment presented in Fig. 2). In order to avoid the introduction of trace quantities of CO into the anode of FC, the TCD reactor was thoroughly purged with ultra-pure Ar for 1 h at operational temperature, and then let run for about an hour on the methane feedstock before introducing the effluent gas to the FC (although the feedstock itself does not contain any oxidants, the trace quantities of CO could possibly originate from oxygen and/or moisture impurities entrained or adsorbed on carbon catalyst surface). Small quantity of ethylene in the effluent gas was converted to ethane by passing it through a hydrogenation reactor (as described above). Fig. 11 shows the performance of the single-cell PEMFC using the H_2–CH_4 mixtures with H_2 concentration of 35 and 46 vol.% produced in the TCD reactor. As in the previous case (see the sub-section 3.2.1) the feed with lower H_2 concentration yielded lower cell voltage in the concentration polarization region. The TCD-FC system ran for several hours (during a quasi-steady state methane decomposition process). The results indicate that PEMFC could be successfully operated on the H_2–CH_4 feed produced by TCD of methane.

4.4. Energy conversion efficiency of integrated TCD-FC power generation systems

The chemical-to-electrical (CTE) energy conversion efficiency of the integrated TCD–H_2FC–DCFC power generation system is defined here as a total electrical energy output from the system (e.g., in kW$_{el}$h) divided by input chemical energy (higher heating value) of hydrocarbon fuel (e.g., in kWh) (in this case, chemi-
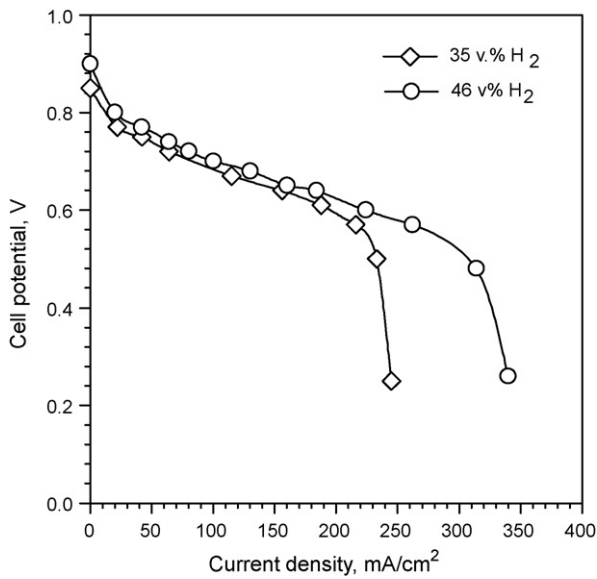
Fig. 11. Performance testing of a single-cell PEMFC using two H_2–CH_4 mixtures produced by the thermocatalytic reactor operating on methane as a feedstock.

cal energy of input fuel covers all thermal and electrical energy requirements of the operational units within the close loop system). Evidently, the overall CTE energy conversion efficiency of the integrated system is controlled by the efficiencies of the TCD reactor, H_2FC and DCFC.

The following calculations provide an estimate of the energy efficiency of the methane-fed TCD process. The calculations are based on the experimental data obtained during steady state decomposition of methane at 880–890 °C over plasma-generated carbon particles (both fixed and moving bed reactor options are considered). The overall energy efficiency (η_{eff}) of methane decom-

position to hydrogen and carbon in the TCD reactor can be defined as follows:

$$\eta_{eff}\ (\%) = \frac{\Delta H_{H_2} + \Delta H_{carbon}}{\Delta H_{CH_4} + \Delta H_{TCD}/\phi + W_{el}/\xi\varphi} \times 100 \qquad (9)$$

where ΔH_{H_2}, ΔH_{carbon}, ΔH_{CH_4} are the higher heating values (HHV) of H_2, carbon and methane, respectively; ΔH_{TCD} is enthalpy of methane decomposition reaction at operational temperature of the reaction; W_{el} is an electrical energy input to the process (e.g., to power the plasma device, if needed); ϕ is the thermal efficiency of the TCD reactor; φ is thermal-to-electrical energy conversion efficiency, and ξ is the electrical efficiency of the plasma device.

It was assumed that methane was used as fuel for the TCD process heat input and for gas-fired turbines to generate electricity with the thermal-to-electrical energy conversion efficiency of $\varphi = 0.4$. To account for the energy losses and inefficiencies in providing the thermal energy to the TCD reactor the thermal efficiency of the TCD reactor was assumed $\phi = 0.85$ (It should be noted that modern catalytic reactors combined with efficient heat recovery/recycling system can achieve up to $\phi = 0.9$ thermal efficiency). Similarly, to account for losses in the non-thermal plasma device, its electrical efficiency was assumed to be $\xi = 0.8$. Note that the share of electrical energy input for powering the plasma device against the total energy input to the TCD process is relatively low (about 10–15%). Based on the above input data and assumptions, the overall energy efficiency of the TCD of methane process was estimated at about 81–85% (depending on heat input options and the system throughput).

The following are the estimates of the overall chemical (methane, propane) to electrical energy conversion efficiencies of the integrated power generation systems combining a TCD reactor with H_2FC and DCFC. In particular, two options for H_2FC were considered: PEMFC (option A), or SOFC (option B). The CTE efficiency estimates are based on the following assumptions (note that FC efficiencies below represent projected values based on the expected
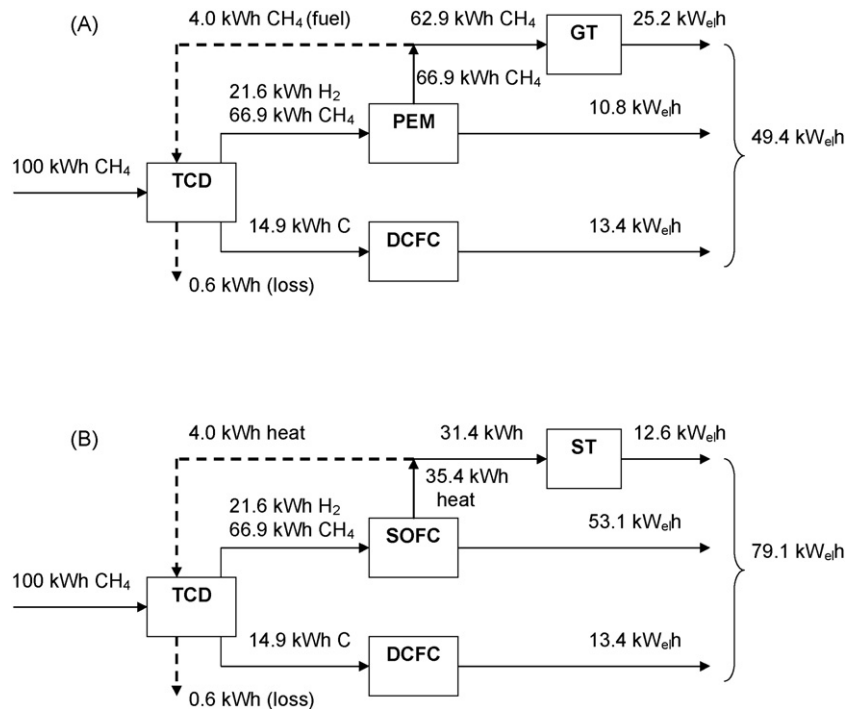

Fig. 12. Estimation of chemical-to-electrical energy conversion efficiency of the integrated TCD–H_2FC–DCFC power generation system using 100 kWh of methane as input fuel. Option A: combination of the TCD reactor with PEMFC and DCFC. Option B: combination of the TCD reactor with SOFC and DCFC. GT: gas turbine and ST: steam turbine.
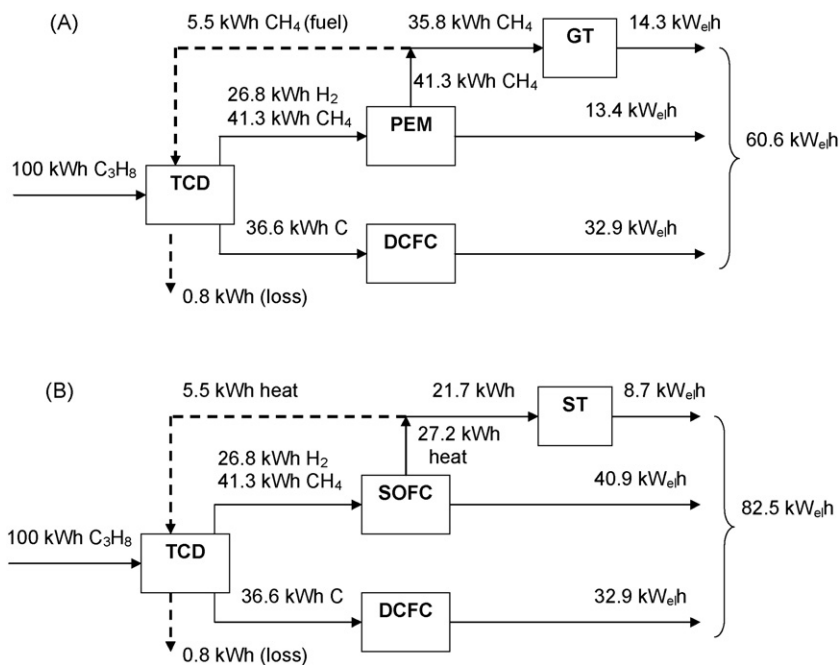
Fig. 13. Estimation of chemical-to-electrical energy conversion efficiency of the integrated TCD–H$_2$FC–DCFC power generation system using 100 kWh of propane as input fuel. Option A: combination of the TCD reactor with PEMFC and DCFC. Option B: combination of the TCD reactor with SOFC and DCFC.

advancement of the technologies):

- TCD reactor temperature: 880–890 °C, energy efficiency: 85%;
- the energy input requirement values for TCD of methane and propane are taken from Fig. 1 and adjusted to the process temperature;
- methane steady state conversion is 33% at 890 °C (energy input to the TCD process is adjusted to this conversion);
- PEMFC temperature: 80 °C, energy conversion efficiency: 50%;
- SOFC temperature: 900 °C, energy conversion efficiency: 60%;
- DCFC temperature: 700–800 °C, energy conversion efficiency: 90%;
- methane from the PEMFC anode exhaust is used as fuel to provide heat input to the TCD process and generate electricity via a gas turbine with energy conversion efficiency of 40%;
- high-temperature heat from SOFC is used to provide a heat input to the TCD reactor and generate electricity via a turbine with the energy conversion efficiency of 40%;
- SOFC can directly utilize methane component of the H$_2$–CH$_4$ mixtures with the same energy conversion efficiency of 60% (It has been reported recently that SOFC was operated on a pure methane feed at 900 °C for about 200 h without any carbon deposition [18]);
- minor energy penalties related to the transport of gases and carbon, heat exchanger losses, etc. are neglected.

Fig. 12 shows the details of the overall CTE energy conversion efficiency calculations for the options A and B based on 100 kWh methane input. Methane conversion of 33% would correspond to H$_2$ concentration of ~50 vol.% in H$_2$–CH$_4$ mixtures, according to the following chemical equation:

$$CH_4 \rightarrow 0.66CH_4 + 0.66H_2 + 0.33C \qquad (10)$$
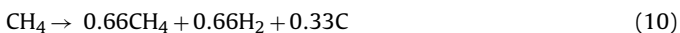
It can be seen that 49.4 kW$_{el}$h of electrical energy could be generated from 100 kWh of methane in the integrated TCD–PEMFC–DCFC system. The use of SOFC results in significant (almost by 30%) CTE efficiency improvement over the option with PEMFC, mostly due to the thermal integration of SOFC with the TCD reactor, and the capa-

bility of SOFC to directly utilize methane component of the H$_2$–CH$_4$ mixtures. The overall CTE efficiency of the TCD–SOFC–DCFC system reaches up to 79.1%, which far exceeds that of the conventional HR-FC systems. If one assumes complete conversion of methane to hydrogen and carbon, the CTE values for the options A and B will increase to 65.9 and 83.7%, respectively (In principle, the methane conversion yield could be significantly increased by switching to other types of moving bed reactors, e.g., fluidized bed reactor, where residence time is easier to control; sustainable methane conversion in excess of 80% is technically feasible upon further improvement of the TCD technology).

One can expect that heavier hydrocarbon fuels (e.g., propane) could yield higher CTE energy conversion efficiency than methane due to the greater share of the carbon component in fuel (C/H atomic ratio in propane is 0.375, compared to 0.25 in methane). The estimates of propane CTE energy conversion efficiency for the options A and B are shown in Fig. 13. The calculations were based on the experimental results related to carbon-catalyzed decomposition of propane (see Fig. 3) (to simplify the calculations, the [H$_2$]/[CH$_4$] ratio in the product gas is taken 2 (v/v), and small quantities of C$_2$ hydrocarbons are neglected). Based on the above ratio of gaseous products of propane decomposition and the measured yield of the carbon product, the TCD of propane process can be approximated by the following chemical equation:

$$C_3H_8 \rightarrow 2H_2 + CH_4 + 2C \qquad (11)$$

It was estimated that the combination of the propane-fed TCD reactor with PEMFC and DCFC would yield the overall CTE energy conversion efficiency of 60.6%, which is a significant increase over the value of 49.4% for methane. The combination of propane-TCD with SOFC and DCFC, however, showed a relatively small improvement (from 79.1 to 82.5%) over the same combination with methane as fuel. This can be explained by the fact that not all carbon from the propane feed ended up in DCFC (however, if we assume complete decomposition of propane to H$_2$ and carbon, then the CTE values for the options A and B would increase to 70.8 and 84.7%, respectively).

One of the advantages of the proposed integrated system relates to its flexibility in terms of producing both energy carriers: hydrogen and electricity. One can see that the integrated scheme can be easily modified to generate electricity (by DCFC) and deliver hydrogen or H_2–CH_4 mixtures (in the former case, H_2 has to be recovered from the mix by a pressure-swing adsorption unit) for a variety of applications. In particular, the H_2–CH_4 mixtures can be used in ICE-based transportation, whereas, pure H_2 (99.999%) is an ideal fuel for PEMFC-based vehicles. The H_2/electricity output ratio of the integrated system can be conveniently controlled by changing the amount of H_2 fuel directed to PEMFC or SOFC.

5. Environmental impact of the technology

Potentially, there are three sources of CO_2 emissions from the integrated TCD–H_2FC–DCFC power generation system: (i) the TCD reactor heated by methane combustion, (ii) SOFC using H_2–CH_4 mixtures as a feed, and (iii) DCFC using carbon fuel. Overall CO_2 emissions from the TCD process depend on the means for providing an energy input to the process. Advantageously, due to relatively low endothermicity of the methane decomposition reaction and the lack of gas conditioning (e.g., water gas shift) and steam generation stages, its energy input requirement (37.8 kJ mole^{-1} H_2) is relatively low compared to conventional SMR process (63.3 kJ mole^{-1} H_2). Assuming that part of un-reacted methane was used as fuel for providing the heat input to the process, the overall CO_2 emissions from the TCD process per unit of hydrogen produced would be:

$$(CO_2)_{TCD} = \frac{W_{el}\psi}{\langle H_2 \rangle} + \frac{\Delta H_{TCD}\mu_{CO_2}}{\langle H_2 \rangle \phi \ \Delta H_{NG}} \left(\frac{gCO_2}{gH_2} \right) \qquad (12)$$

where $(CO_2)_{TCD}$ is CO_2 emission from TCD process, ψ is CO_2 emissions resulting from generation of electrical power, μ is molecular weight of CO_2 ($\mu = 44$), $\langle H_2 \rangle$ is hydrogen yield per unit of methane.

Based on the above formula, the CO_2 emissions from methane-TCD process are estimated at 1.8–2.8 g CO_2 g^{-1} H_2 (depending on the share of electrical energy input to the TCD process), which is at least 3–4 times less than that from conventional SMR process (9.7 g CO_2 g^{-1} H_2 [19]). If the TCD reactor is thermally integrated with SOFC, CO_2 emissions from the reactor would significantly drop (but will not be completely eliminated, because SOFC is fed by H_2–CH_4 mixtures). The overall CO_2 emissions from the methane- and propane-based integrated TCD–H_2FC–DCFC power generation systems are estimated to be in the range of 0.26–0.41 kg CO_2 per kW$_{el}$h (depending on the specific configuration of the system). For the comparison, CO_2 emissions per kW$_{el}$h produced from electric power generation sources in U.S. (including fossil and non-fossil sources) amount to 0.61 kg CO_2 per kW$_{el}$h [20]. Advantageously, most of CO_2 byproduct from the integrated power generation system originates from DCFC (and partially from SOFC) in the form of concentrated CO_2 stream, ready for sequestration, thus, obviating the need for energy intensive CO_2 capture and purification operations (which would significantly improve the process economics).

6. Conclusions

The objectives of this work are threefold: (i) to develop continuous (or sustainable) thermocatalytic hydrocarbon decomposition process for CO_x-free production of hydrogen-rich gas and carbon, (ii) to test the thermocatalytic hydrocarbon decomposition reactor in combination with PEMFC to verify that the latter can operate on H_2–CH_4 mixtures produced by the reactor, and (iii) to analyze the integrated power generation system including a thermocatalytic hydrocarbon decomposition reactor combined with a direct carbon and hydrogen FC, and estimate its overall chemical-to-electrical energy conversion efficiency. Two types of hydrogen-fueled FC

were considered for the analysis: low-temperature (PEMFC) and high-temperature (SOFC) fuel cells.

A thermocatalytic NG decomposition reactor coupled with a sulfur scrubber, hydrogenation and methanation reactors for the production of sulfur-free H_2–CH_4 mixtures with permissible levels of CO (<10 ppmv) suitable for PEMFC operation has been constructed and tested. It was demonstrated that hydrogen-rich gas with the H_2 concentrations in the range of 35–50 vol.% (balance methane) could be continuously produced from pipeline-quality NG. Carbon produced by thermocatalytic decomposition of hydrocarbons was characterized and its structure was found to be consistent with that of semi-ordered (or turbostratic) carbon. The reported literature data indicate that this type of carbon exhibits high electrochemical activity in direct carbon FC.

A four-cell PEMFC stack was assembled and operated using H_2–CH_4 mixtures of different compositions (40–100 vol.% H_2). It was shown that the presence of methane in the anode feed did not adversely affect the performance of PEMFC beyond an ordinary dilution effect. PEMFC was successfully tested using H_2–CH_4 mixtures produced by TCD of methane. It was estimated that overall chemical-to-electrical energy conversion efficiency of the integrated TCD–H_2FC–DCFC systems could vary in the range of 49.4–82.5%, depending on the type of fuel and hydrogen FC used. CO_2 emission per kW$_{el}$h produced by the integrated system is about half of that from conventional power generation sources. Advantageously, CO_2 is produced in concentrated sequestration-ready form, which obviates the need for a costly and energy intensive capture of CO_2.

Acknowledgements

References

[1] C. Thomas, B. James, F. Lomax, I. Kuhn, Int. J. Hydrogen Energy 25 (2000) 551–567.
[2] A. Avchi, I. Onsan, D. Trimm, Appl. Catal. A: Gen. 216 (2001) 243.
[3] L. Pettersson, R. Westerholm, Int. J. Hydrogen Energy 26 (2001) 243–264.
[4] U.S. DOE, Hydrogen, Fuel Cells & Infrastructure Technologies Program, U.S. Department of Energy, Office of Energy Efficiency and Renewable Energy, Washington DC, 2003.
[5] S. Zecevic, E. Patton, P. Parhami, Carbon 42 (2004) 1983–1993.
[6] D. Cao, Y. Sun, G. Wang, J. Power Sources 167 (2007) 250–257.
[7] M. Steinberg, J. Cooper, N. Cherepy, Proceedings of the AIChE 2002 Spring Meeting, New Orleans, 2002, pp. 2112–2127.
[8] H. Saito, S. Hasegawa, M. Ihara, J. Electrochem. Soc. 155 (2008) B443–B447.
[9] N. Cherepy, R. Krueger, K. Fiet, A. Jankowski, J. Cooper, J. Electrochem. Soc. 152 (2005) A80–A87.
[10] S. Jain, J. Lakerman, K. Pointon, J. Irvine, Trans. ASME 4 (2007) 280–282.
[11] N. Muradov, F. Smith, Catal. Today 102–103 (2005) 225–233.
[12] A. Czernichowski, P. Czernichowski, A. Ranaivosolarimanana, Proceedings of the 11th World Hydrogen Energy Conference, Stuttgart, Germany, 1996, p. 661.
[13] N. Muradov, F. Smith, G. Bokerman, J. Phys. Chem. C 113 (2009) 9737–9747.
[14] U.S. Department of Energy, FreedomCar and Fuel Technical Partnership, www1.eere.energy.gov/vehiclesandfuels/about/partnerships/freedomcar/fc_goals.html.
[15] H. Hiller, et al. (Eds.), Ullmann's Encyclopedia of Industrial Chemistry, Gas Production, Wiley–VCH Verlag GmbH & Co., 2002.
[16] D. Hirsch, A. Steinfeld, Int. J. Hydrogen Energy 29 (2004) 47–55.
[17] J. Hirschenhofer, D. Stauffer, R. Engleman, M. Klett, Fuel Cell Handbook, Fourth ed., 1998, DOE/FETC-99/1076.
[18] J. Klein, M. Henaut, C. Roux, Y. Bultel, S. Georges, J. Power Sources 193 (2009) 331–337.
[19] P. Spath, M. Mann, Life cycle assessment of hydrogen production via natural gas steam reforming, Technical Report, NREL, NREL/TP-570-27637, 2000.
[20] Carbon dioxide emissions from the generation of electric power in the United States, US DOE and EPA Report, July 2000.